Applied Engineering
2018; 2(2): 39-53
http://www.sciencepublishinggroup.com/j/ae
doi: 10.11648/j.ae.20180202.13

Performance Improvement of a Dry Mode Natural Gas Fired Turbine Plant for Combined Cycle Operation

Anthony Kpegele Le-ol[1, *], Duabari Silas Aziaka[2]

[1]Department of Mechanical Engineering, Rivers State University, Port Harcourt, Nigeria
[2]Center for Power and Propulsion, Cranfield University, Bedfordshire, United Kingdom

Email address:
le-ol.anthony@ust.edu.ng (A. K. Le-ol), d.aziaka@cranfield.ac.uk (D. S. Aziaka)
[*]Corresponding author

To cite this article:
Anthony Kpegele Le-ol, Duabari Silas Aziaka. Performance Improvement of a Dry Mode Natural Gas Fired Turbine Plant for Combined Cycle Operation. *Applied Engineering*. Vol. 2, No. 2, 2018, pp. 39-53. doi: 10.11648/j.ae.20180202.13

Received: September 17, 2018; **Accepted**: November 5, 2018; **Published**: December 3, 2018

Abstract: This research considers the design of combined cycle (CC) operation for a dry mode natural gas fired turbine plant in southern Nigeria. It entails evaluation and utilization of the amount of waste heat energy exhausted by the Omoku gas turbine (GT) power plant by integrating a steam Rankine cycle retrofitted with a heat recovery steam generator (HRSG) for CC operation, with the focus to improving its performance and reducing waste heat intensity to the environment. Gathered data from the human machine interface (HMI) and log sheets were used for the analysis. Thermodynamic sensitivity analysis was implemented for the combined cycle system (CCS) using a developed model in the MATLAB platform. The outcome of energy balance of the HRSG having a heat load of 38.49 MW showed that for every kg of exhaust gas, 0.1164 kg of steam is generated at an optimum pressure of 40 bar and mass flow of 14.45 kg, with acceptable steam turbine exhaust moisture content of 10%. These revealed a quantified amount of 45.28 MW heat energy contained in the usually wasted exhaust gas of the dry mode GT which was thus recovered in the HRSG, producing additional 16.32 MW as the steam turbine (ST) power output with a feed pump heat load of 0.06 MW and a condenser heat load of 28.96 MW. Further analysis in terms of power outputs, energy efficiencies, and environmental impacts showed that the CCS achieved 41.32 MW, 49.26% and HRSG stack temperature of 170.25°C compared to the previously 25 MW, 26.60% and exhaust gas temperature (EGT) of 487°C respectively of the dry mode GT. These indicate that the CCS generates about 65.30% boost in the net power output, 85.20% improvement in overall efficiency and 65.10% reduction in waste heat intensity to the environment when compared with the dry mode GT operating in isolation. Thus, the work showed that for the design of a CCS with a single pressure level HRSG without supplementary firing, a recommended range for the power output of the steam bottoming plant falls within 34 – 40% of the total power output of the CCS while that of the gas topping plant falls within the range of 60 – 66% of the total power output of the CCS. This study therefore confirms the viability as well as demonstrates the application, of the combined cycle concept for the Omoku gas turbine and recommends for further research, the introduction of a multiple pressure level HRSG with supplementary firing to the combined cycle system for an improved efficiency and output.

Keywords: Dry Mode Gas Turbine, Combined Cycle System, Heat Recovery Steam Generator, Waste Heat Intensity, Heat Load, Power Output

1. Introduction

1.1. Background of the Study

Combined cycle (CC) operation is one of the most efficient alternative ways to exploit the available heat energy in the wasted exhaust gas of a dry mode gas turbine (GT) for performance enhancement. The dry mode gas turbine is a conventional device for converting thermal energy through mechanical energy to electrical power [1]. Gas turbines are generally, widely used for producing electricity and various other industrial activities. They can be used in stationary power plants as the topping cycle to generate electricity as stand-alone units or in conjunction with steam turbine as the bottoming power plant either as cogeneration or combined cycle gas turbine where the exhaust gas serves as a heat source for the steam [2]. A simple gas turbine discards most of the added heat into the atmosphere with temperatures in the range of 430 to 590°C. These temperatures are higher than the operating temperatures in the steam cycle and some of the wasted energy could be recovered in a Heat Recovery Steam Generator (HRSG) [3]. It is observed that considerable amount of heat energy goes as a waste with the exhaust gas of an open cycle gas turbine accompanied with disastrous emission to the environment which has been a great concern due to their impact on human health, nature and materials. Thus, energy conversion and supply are a key driver of the many negative environmental trends in the world today as the burning of fossil fuels generates CO_2 and other greenhouse gases that are responsible for global warming which results to climatic change and thermal pollution [4].

Lebele-Alawa and Le-ol [5] in their work; noted that a combined cycle power plant (CCPP) is a power plant where electricity production is done from the combination of both gas and steam turbines. The gas turbine called topping cycle burns fuel and operates at high average temperatures, a second cycle called bottoming cycle utilizes the exhaust energy from the gas turbine, which also is quite high, to produce steam. The topping and bottoming cycles is coupled with a waste heat recovery steam generator that transfers heat [6]. Thus, the CCPP is a system in which a gas topping plant operating on Brayton cycle at a higher temperature to generate electricity is coupled through the HRSG to a steam bottoming plant operating on Rankine cycle at a reduced temperature generating additional electric power. By this combination, the average temperature of the rejected heat is reduced when compared with that of the gas turbine operating in isolation and the average temperature of heat addition increases above that of a single steam turbine operating alone [7]. Thus, the overall thermal efficiency of the combined cycle is higher compared to the individual efficiencies of the gas or steam turbine cycles operating separately. This higher efficiency results from the utilization of the same fuel to provide heat and electricity, thereby reducing fuel consumption and compensating fuel cost which in turn reduce emission levels as less fuel is fired per unit power produced [8]. Lars & Bolland [9] observed in their work that the addition of a steam bottoming cycle to the gas turbine topping cycle, making it a combined cycle is one alternative to increasing the efficiency of the power plant, and thereby decreasing the CO_2 tax per generated MW. This is in line with the analysis of Lebele-Alawa and Le-ol [5] as it was observed that retrofitting a steam bottoming plant to a 25 MW gas turbine enhanced performance with about 51% boost in the net power output and 84% improvement in the overall efficiency.

Polyzakis *et al*., [10] performed the optimization of a combined cycle power plant describing and comparing four different gas turbine cycles: simple cycle, intercooled cycle, reheated cycle and intercooled and reheated cycle. The results showed that the reheated gas turbine is the most desirable over all mainly because of its high turbine exhaust gas temperature and resulting high thermal efficiency of the bottoming steam cycle. The optimal gas turbine led to a more efficient combined cycle power plant (CCPP), and results to great savings. Tiwari *et al*., [11] in their work on ''the effect of operating parameters on combined cycle performance'' observed that the CCPP achieved efficient, reliable and economic power generation. They further stated that the major operating parameters which influence the combined cycle are; turbine inlet temperature, compressor pressure ratio, pinch point, ambient temperature and pressure levels. Again, the work of Ravi *et al*., [12] and Murad *et al*., [13] discussed the effect of various parameters like pinch point, approach point, steam pressure, steam temperature, gas flow rate on the performance of the (HRSG). Ahmed [14] noted that the mass flow rate of steam and steam temperature in a combined cycle system depends on the amount of heat available in the gas turbine exhaust. Thamir & Rahman [15] did a parametric thermodynamic analysis of a combined cycle investigating the effect of operating parameters on the overall plant performance. The simulation results showed that the overall efficiency increases with the increase of the peak compression ratio. The overall thermal efficiencies for CCPP are higher compared to that of the gas-turbine plants.

This work therefore considers the evaluation and utilization of the amount of waste heat energy exhausted by Omoku simple cycle Gas turbine (dry mode gas turbine) for CC operation. The focus is to improve performance and reduce waste heat intensity to the environment. It entails integrating a steam rankine cycle retrofitted with a heat recovery steam generator (HRSG) to the existing dry mode GT making it a combined thermal power plant (CTPP). The outcome of the study will be the design of efficient and cost-effective energy system within the specification of environmental conditions.

1.2. Experimental Engine Description (Omoku Gas Turbine Power Plant)

The experimental engine used for this research is the Omoku Gas Turbine power plant, located at Onelga, the Northern part of Rivers State, Southern coastal area of Nigeria. The location geographic coordinates in World Geodetic System (WGS 84) lies on Longitude: 6°39′24″ E and Latitude: 5°20′37″ N at 18m (59 ft) elevation above sea level, experiencing an equatorial temperature of 24°C, relative humidity of 97% and South-West wind at 2 km/h.

The ENGINE model is a MS5001PA. It is a 25 MW capacity dry mode MS 5001 (GE Frame 5), single shaft generator drive industrial gas turbine with seventeen stages of axial compressor and a two stages axial turbine with constant mean diameter annular configuration, operating with a combustor exit temperature of 1232 K, overall pressure ratio of 10, mass flow of 122.9 kg/s, 5202 rpm maximum shaft output speed, at ISO conditions with generator coupled at the cold end drive and exhaust gas temperature of 487°C [16].

The Omoku gas turbine power plant is an open cycle (dry mode) gas turbine and thus, operates on the principles of Brayton cycle. It consists of a compressor, a combustion chamber and a gas turbine driving a generator to produce electricity. Instead of flaring the hot exhaust gas from this

Brayton cycle plant, this heat was utilized by incorporating a heat recovery steam generator (HRSG) to generate superheated steam to drive a retrofitted steam turbine, making it a combined cycle system (CCS) thus producing additional power output resulting in an improved efficiency and power output. These reasons prompted the need in this research for the performance improvement of the Omoku gas turbine power plant for combined cycle operation. Figure 1 shows the gas turbine package flow diagram, figure 2 shows the HMI schematic diagram and figure 3 is a pictorial view, all of the Omoku gas turbine.

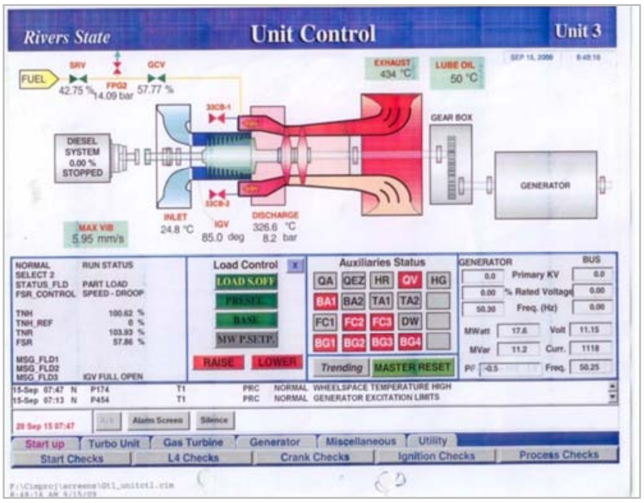

Figure 1. Major Sections of the MS5001 Gas Turbine (Omoku Gas Turbine) Assembly [16].

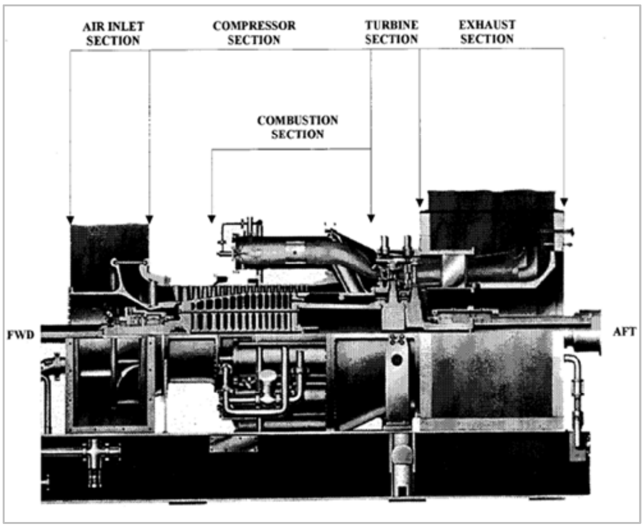

Figure 2. HMI Schematic Diagram of Omoku Gas Turbine Operation.

Source: Omoku Gas Turbine Manufacturer's Manual Source: Omoku Gas Turbine Plant Control Room

2. Materials and Methods

2.1. Data Collection and Modeling Software

The materials required for the research were technical data from the Omoku Gas turbine power plant collected through direct observation from the monitoring screen of the human machine interface (HMI) as well as log sheets and manufacturer's manuals. The parameters monitored included inlet and exit temperatures and pressures of the components, and air and exhaust gas flow rates. Other parameters which cannot be directly measured were calculated, using standard thermodynamic relations. To analyze the proposed CCPP, there was a need to know the amount of exhaust gases and temperature required to generate certain amount of steam. These were achieved by carrying out heat balance on the HRSG applying pinch technology and iterating the live steam pressure at different conditions from 100 to 3 Bar. Using standard thermodynamic equations implemented with MATLAB software (MathWorks, USA), the appropriate parameters of the various components of the steam turbine power plant were determined and thus the net power output and overall efficiency of the combined cycle plant.

Figure 3. Pictorial View of Omoku Gas Turbine Power Plant.

2.2. System Modeling of the Proposed Combined Cycle System

A combined gas and steam cycle system is proposed for the effective utilization of the waste flue gas liberated by the Omoku GT. The proposed retrofitted combined-cycle system unit consists of the Brayton cycle (the dry mode Omoku gas turbine) and a Rankine cycle (the retrofitted steam turbine) incorporated by a HRSG comprising of an economizer, evaporator, and superheated. Figure 4 shows the schematic diagram of the retrofitted combined cycle system.

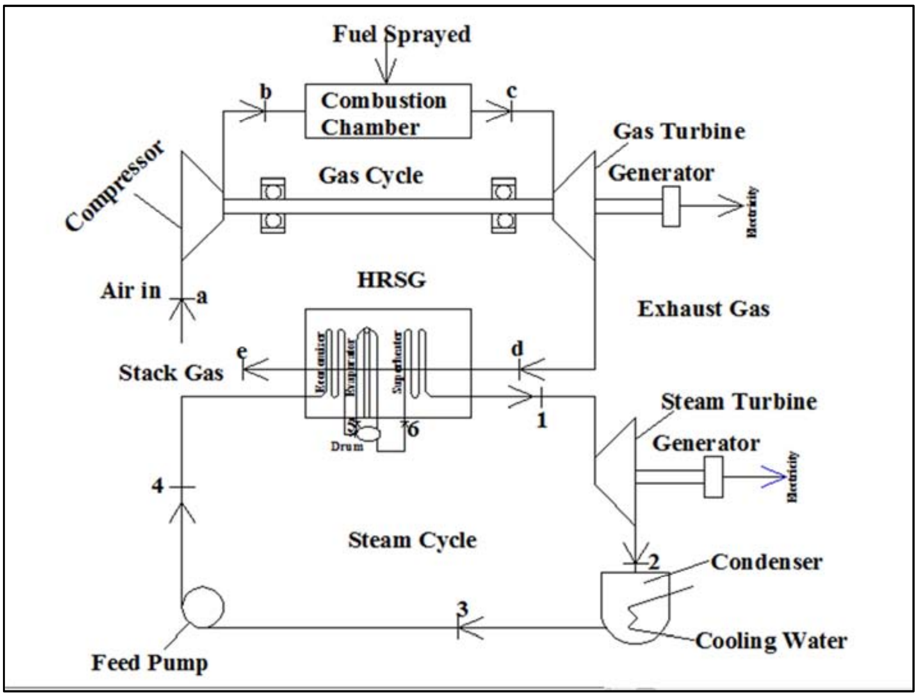

Figure 4. *Schematic Diagram of the Retrofitted Combined Cycle System.*

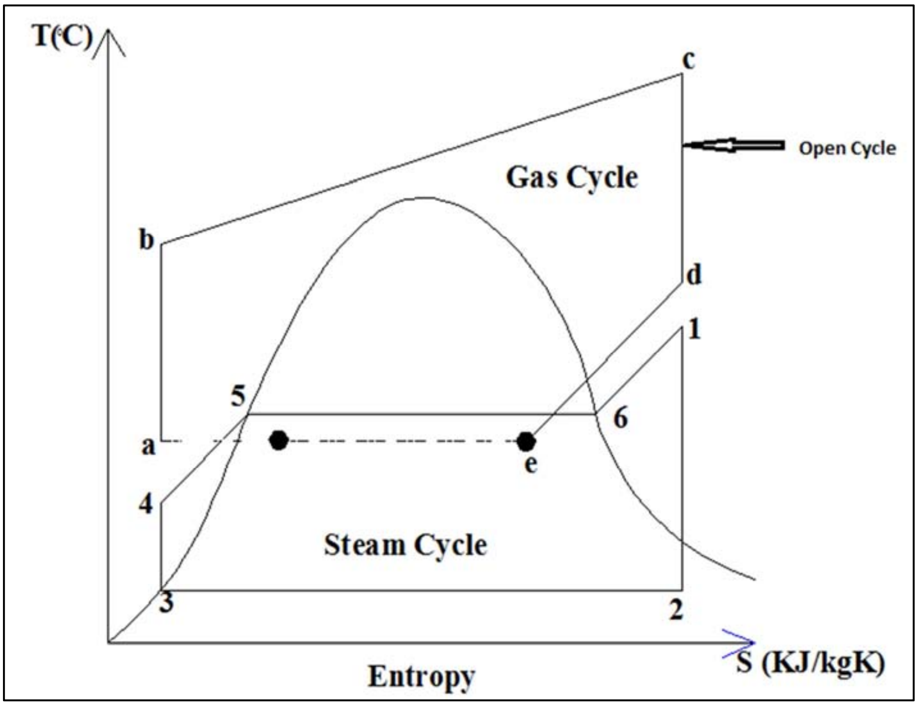

Figure 5. *Temperature Entropy Diagram of the Retrofitted Combined Cycle.*

The temperature-entropy diagram analyzing the degree of randomness at every stage in the combined cycle is shown in Figure 5. The heat from the exhaust of the gas-topping cycle is used to generate superheated steam for the steam-bottoming cycle which thus provides additional electricity. The different thermodynamic processes occurring in the system are:

Processes a→ b → c → d ≡ Omoku Gas turbine Cycle (GTC)

Processes 1 → 2 → 3 → 4 → 1 ≡ Retrofitted Steam Turbine Cycle (RSTC)

Processes 4 → 5→ 6 → 1 ≡ Heat Recovery Steam Generator (HRSG)

Process d → e ≡ heat transfer from exhaust gas of gas topping cycle to the HRSG of the steam bottoming cycle

2.2.1. Gas Topping Cycle (Dry Mode Omoku Gas Turbine)

The Brayton configuration is utilized in the Omoku gas turbine power plant. This is represented by the Cycle ≡ a→ b

→ c → d on T – S diagram of the proposed Retroffited Combined Cycle System in figure 5. The schematic diagram indicating the isentropic processes of the GTC is shown in Figure 6.

Table 1 displays the necessary data required for the performance analysis of the power plant which equally served as the input data for the design/conversion to a combined cycle.

Table 1. *Omoku Gas Turbine Plant Main Characteristics (Average Input Data for CCS).*

Component	Parameter	Symbol	Unit	Value
	Inlet temperature	T_1	°C	30.4
Turbo compressor	Outlet temperature	T_2	°C	367
	Inlet pressure	P_1	bar	1.013
	Outlet pressure	P_2	bar	10
	Mass flow rate (Air)	$\dot{m}_a$	kg/s	122.9
Combustion chamber	Fuel consumption (flow rate)	$\dot{m}_f$	kg/s	1.2
	Inlet temperature	T_3	°C	959
Turbine	Outlet temperature	T_4	°C	487
	Exhaust gas flow (flow rate of gas)	$\dot{m}_{eg}$	kg/s	124.1
Other data	Thermal efficiency	$\eta_{th_{gT}}$	%	26.6
	GT Power output	P_{gT}	MW	25

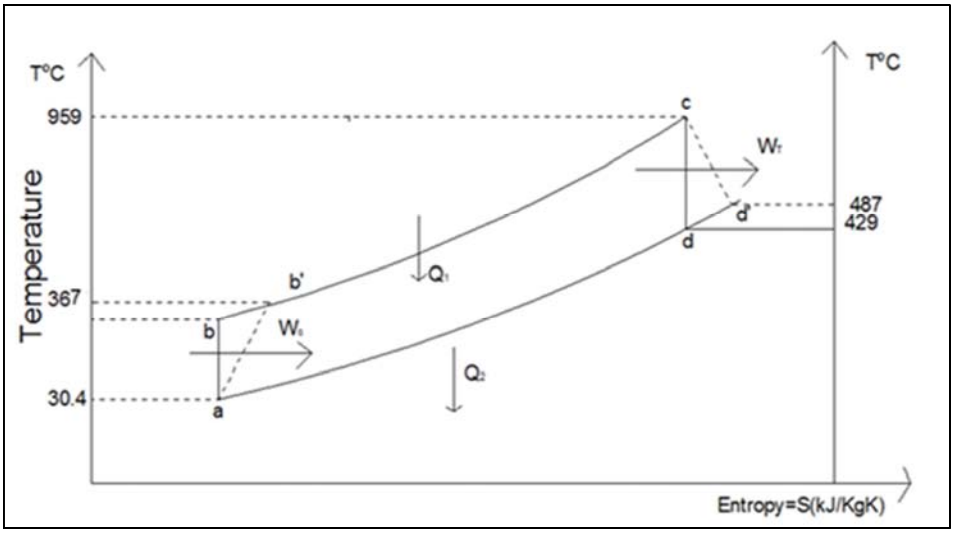

Figure 6. *Omoku Gas Turbine Cycle on T-S Diagram Showing Isentropic Process.*

The energy balance of the brayton cycle is modeled as follows:

The air at ambient temperature enters the compressor at point a, exits the compressor at a temperature T_b calculated with:

$$\frac{T_b}{T_a} = \left(\frac{P_b}{P_a}\right)^{\gamma-1/\gamma} \quad (1)$$

Where T_a *and* T_b are the entry and exit air temperatures of the compressor; P_a *and* P_b are the air pressures before and after compression process while γ is the specific heat ratio.

Applying steady flow, the model energy equations yield

$$\text{Heat supplied } \dot{Q}_1 = \dot{m}_{eg} c_{p_{eg}} (T_c - T_{b^1}) \quad (2)$$

$$\text{Heat rejected: } \dot{Q}_2 = \dot{m}_{eg} c_{p_{eg}} (T_{d^1} - T_a) \quad (3)$$

Where $\dot{m}_{eg} = Exhaust\ gas\ flow$, $c_{p_{eg}} = Specific\ heat\ at\ constant\ Pressure\ of\ exhaust\ gas\ (\ CO_2\ )\ at\ EGT$

Compressor Power: $P_c = \dot{m}_a c_{p_a} (T_{b^1} - T_a)$ (4) Where c_{p_a} = specific heat at constant pressure of air at compressor outlet tem p.

$$\text{Turbine Power: } P_T = \dot{m}_{eg} c_{p_{eg}} (T_c - T_{d^1}) \quad (5)$$

$$\text{Gas Turbine Power Output: } P_{NET} = P_T - P_C \quad (6)$$

$$\text{Gas Turbine Cycle Thermal Efficiency: } \eta_{thgT} = \frac{Net\ Power\ Output}{Heat\ Supplied} = \frac{P_{NET}}{\dot{Q}_1} \tag{7}$$

$$\text{Turbine Isentropic Efficiency: } \eta_{isgT} = \frac{T_c - T_{d1}}{T_c - T_d} = \frac{Actual\ Work}{Isentropic\ Work} \tag{8}$$

2.2.2. Heat Recovery Steam Generator (HRSG)

The HRSG consists of three heat exchanger sections namely the economizer, the evaporator, and the superheated [7].

Figures 7 & 8 show typical schematics of a Single Pressure HRSG system and the temperature-heat diagram of a single-pressure level respectively, for a combined cycle.

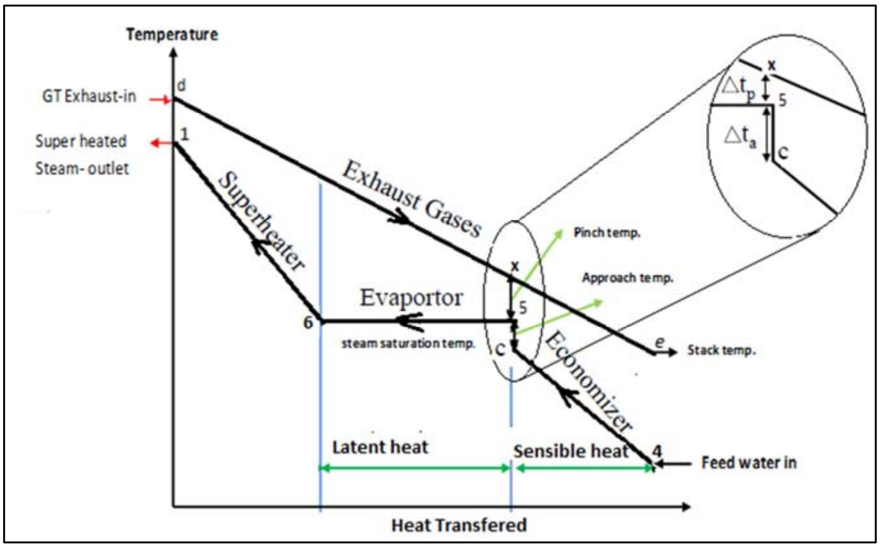

Figure 7. *Typical schematic of a Single Pressure HRSG system.*

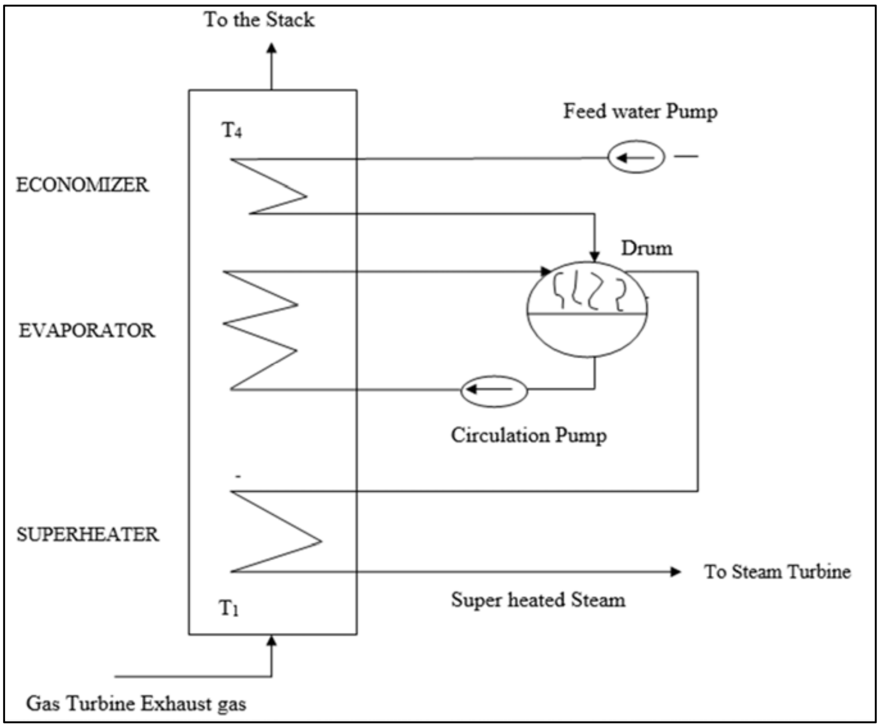

Figure 8. *Temperature Heat diagram for a Single Pressure HRSG thermodynamic Model.*

The temperature of the steam increases from point 4 to 1 where process 4 – 5 represents the economizer; process 5 – 6 represents the evaporator, and process 6 – 1 is the superheater. The exhaust gas is cooled from point T_d of the gas turbine to a temperature of T_e well above its acid dew point temperature.

Two important design parameters of a HRSG are the Approach temperature difference denoted as ΔT_a and the

Pinch-point temperature difference denoted as ΔT_p..

For a pinch-point temperature difference of ΔT_p, the pinch-point on the gas side is;

$$T_x = T_5 + \Delta T_p \quad (9)$$

Similarly, the economizer outlet temperature can be evaluated using

$$T_c = T_5 + \Delta T_a \quad (10)$$

The HRSG ratings were determined employing heat balance formulations from the GT exhaust to the HRSG, as given by the simultaneous equations:

$$\dot{m}_{eg} c_{peg}(h_1 - h_4) = \dot{m}_{eg} c_{peg}(T_d - T_e) \quad (11)$$

$$\dot{m}_s(h_5 - h_4) = \dot{m}_{eg} c_{peg}(T_x - T_e) \quad (12)$$

$$T_e = \frac{T_x(h_1 - h_4) - T_d(h_5 - h_4)}{h_1 - h_5} \quad (13)$$

Where;

$\dot{m}_s$ = Mass flow rate of steam in kg/s

$\dot{m}_{eg}$= Mass flow rate of exhaust gas in kg/s

T_e = HRSG stack temperature (Exhaust gas cooling temperature)

T_x = Pinch point exhaust gas temperature

T_d= Gas turbine outlet (exhaust) temperature

c_{peg}= Specific heat of exhaust gas

2.2.3. Rankine Cycle (Retrofitted Steam Turbine)

The retrofitted Steam turbine to the dry mode Omoku gas turbine operates on the principles of the Rankine cycle. This is represented by the cycle, 1 → 2 → 3 → 4 → 1 on figure 5.

Neglecting changes in kinetic energy (K. E) and potential energy (P. E), application of the steady flow energy equation to the processes reduces to:

$$Q - W = \dot{m}_s \Delta h \quad (14)$$

Hence;

$$\text{Heat supplied in the boiler,} \dot{Q}_2 = \dot{m}_s (h_1 - h_4) \quad (15)$$

$$\text{Heat rejected in the condenser } \dot{Q}_3 = \dot{m}_s (h_2 - h_3) \quad (16)$$

$$\text{Turbine Power } P_{ST} = \dot{m}_s(h_1 - h_2) \quad (17)$$

$$\text{Pump work } P_p = \dot{m}_s(h_4 - h_3) \quad (18)$$

$$\text{Steam Turbine net power output } P_{NET_{ST}} = P_{ST} - P_P \quad (19)$$

$$\text{Steam Turbine Cycle efficiency } \eta_{ST} = \frac{P_{NET_{ST}}}{\dot{Q}_2} = \frac{(h_1 - h_2) - (h_4 - h_3)}{(h_1 - h_4)} \quad (20)$$

$$\text{Note: } h_4 = h_3 + v_f(P_4 - P_3) \quad (21)$$

2.2.4. Condenser Cooling Water System

For the purpose of this design, the inlet temperature difference was taken as 16°C and the pinch point of 10°C was taken as the exit temperature difference resulting to a cooling water temperature rise of 6°C is chosen.

The rate of heat transfer from condensing vapour to the cooling water was determined using equation

$$\dot{Q}_3 = \dot{m}_s (h_2 - h_3) \quad (22)$$

Where $\dot{Q}_3$ = Heat rejected in the condenser known as the Condenser Heat Load.

For energy balance between the condenser and the cooling water system,

$$\dot{m}_w c_{pw}(t_{out} - t_{in}) = \dot{m}_s (h_2 - h_3) = \dot{Q}_3 \quad (23)$$

$$\dot{m}_w = \frac{\dot{Q}_S}{c_{pw}(t_{out} - t_{in})} \quad (24)$$

Where $\dot{m}_s$= Mass flow rate of steam in kg/s

$\dot{m}_w$ = Mass flow rate of cooling water

c_{pw} = Specific heat of water

t_{in} = Temperature of cooling water into condenser

t_{out} = Temperature of cooling water out of the condenser

The condenser Thermal Ratio

$$\eta_{ST} = \frac{Actual\ temp.rise\ of\ cooling\ water}{Maximum\ temp.rise\ of\ cooling\ water} = \frac{t_{out} - t_{in}}{T_2 - t_{in}} \quad (25)$$

Where T_2= condenser saturated temperature

$$\text{Specific Steam Consumption } S.S.C = \frac{1}{w_{net}} \quad (26)$$

Where w_{net}= net work output.

2.2.5. Combined Gas and Steam Cycle Analytical Model

To design the combined gas and steam cycle, there is need to know the amount of exhaust gases and temperature required to generate certain amount of steam so as to be able to calculate the overall thermal efficiency of the combined cycle. These were achieved by carrying out heat balance on the HRSG (heat exchanger).

Treating the HRSG as an adiabatic heat exchanger, the steady flow energy equation becomes:

Energy entering HRSG = Energy leaving HRSG

$$\dot{m}_{eg} c_{peg} T_d + \dot{m}_s h_4 = \dot{m}_{eg} c_{peg} T_e + \dot{m}_s h_1 \quad (27)$$

$$\text{Hence,} \dot{m}_s = \frac{\dot{m}_{eg} c_{peg}(T_d - T_e)}{h_1 - h_4} \quad (28)$$

$$\text{Heat rejected by exhaust gas: } \dot{Q}_{eg} = \dot{m}_{eg} c_{peg}(T_d - T_e) \quad (29)$$

$$\text{The HRSG Thermal Ratio } \eta_{HRSG} = \frac{Q_{HRSG}}{Q_{eg}} \quad (30)$$

$$\text{Hence, HRSG Capacity } Q_{HRSG} = \eta_{HRSG} \dot{Q}_{eg} \quad (31)$$

The combined-cycle overall efficiency and power output are given by:

$$\eta_{CC} = \eta_{ST} + \eta_{gT} - \eta_{ST}\eta_{gT} \quad (32)$$

$$P_{CC} = P_{ST} + P_{gT} \quad (33)$$

Where η_{CC} *and* P_{CC} are combined cycle overall efficiency and power output respectively.

P_{ST} = Steam turbine power output, P_{gT} = gas turbine power output
η_{ST} = Steam turbine thermal efficiency
η_{gT} = Gas turbine thermal efficiency

2.3. Design Considerations for the Proposed Combined Cycle

The designing process of the HRSG and steam turbine was initiated by using the exhaust gas temperature of the GT as the HRSG inlet temperature and assuming values for: the steam turbine inlet temperature (a superheated temperature below the gas turbine EGT), the condenser pressure, and the pinch point and approach temperature while the steam turbine inlet pressures were iterated at different conditions.

Whereas thermal ratio of heat exchanger (HRSG) falls within the range of 75 – 85%, and for which 85% was chosen for this design, the typical steam turbine outlet pressure in condensing mode (condenser pressure) ranges from 0.03 to 0.25 bar [17, 18] and an average value of 0.1 bar was used in this work.

To effectively harness heat from the HRSG so as to have a higher combined cycle thermal efficiency, the stack temperature should be greatly reduced however, above the acid dew point of the flue gas to avoid condensation. Acid dew point of exhaust gas ranges within the values of 104°C - 160°C [19], while pinch point is usually between 8°C and 15°C and approach temperature is in the range 8°C - 12°C [3]. Hence, the combined cycle system was designed for an exhaust gas cooling temperature (HRSG stack temperature) above 160°C chosen as the design point to avoid condensation of the exhaust gas at its acid dew point while a pinch point and approach temperatures of 10°C was used in order to minimize heat loss between the exhaust gas and the steam, and at the same time ensure heat transfer for maximum power output, considering a single pressure level HRSG without supplementary firing. The inlet temperature difference between the condenser and the cooling water was taken as 16°C and a pinch point of 10°C was taken as the exit temperature difference resulting to a cooling water temperature rise of 6°C as chosen.

3. Combined Cycle System Analysis / Results

The results from the application of heat balance on the HRSG utilizing pinch technology and iterating the live steam pressure at twelve different conditions from 100 to 3 bar, using standard thermodynamic equations implemented with MATLAB software is tabulated in Table 2, from which the design specifications for the proposed combined cycle system is stipulated in Table 3.

Table 2. *Results of Combined Cycle Analysis Extracted from MATLAB Model.*

Moisture Content (%)	P_1 [bar]	T_e [°C]	$\dot{Q}_{eg}$ [MW]	Q_{HRSG} [MW]	H_L [MW]	$\dot{m}_s$ [kg/s]	P_P [MW]	P_{ST} [MW]	$P_{NET_{ST}}$ [MW]
22	100.00	211.78	39.35	33.44	5.91	12.95	0.13	15.66	15.53
20	90.00	206.53	40.10	34.08	6.02	13.13	0.12	15.79	15.67
18	80.00	201.01	40.89	34.75	6.14	13.31	0.11	15.94	15.83
16	70.00	194.71	41.79	35.52	6.27	13.53	0.10	16.05	15.96
14	60.00	187.55	42.81	36.39	6.42	13.80	0.08	16.20	16.11
12	50.00	179.43	43.97	37.38	6.59	14.10	0.07	16.29	16.21
10	40.00	170.25	45.28	38.49	6.79	14.45	0.06	16.38	16.32
8	30.00	159.12	46.88	39.84	7.04	14.89	0.05	16.36	16.31
6	20.00	145.12	48.88	41.55	7.33	15.45	0.03	16.20	16.17
4	10.00	124.94	51.76	44.00	7.76	16.29	0.02	15.57	15.56
2	5.00	108.63	54.09	45.98	8.11	16.99	0.01	14.57	14.56
0	3.00	98.58	55.53	47.20	8.33	17.41	0.01	13.71	13.70

Table 2. *Continue.*

Moisture Content (%)	η_{ST} [%]	SSC [kg/s]	$\dot{Q}_3$[MW]	$\dot{m}_w$[kg/s]	η_{cond} [%]	P_{NETgT} [MW]	η_{gT} [%]	P_{CC} [MW]	η_{CC} [%]
22	46.44	8.34	23.82	949.35	37.5	25	26.6	40.53	60.69
20	45.98	8.38	24.43	973.67	37.5	25	26.6	40.67	60.35
18	41.55	8.41	25.05	998.74	37.5	25	26.6	40.83	56.98
16	37.92	8.48	25.83	1029.7	37.5	25	26.6	40.96	54.37
14	35.28	8.56	26.7	1064.2	37.5	25	26.6	41.11	52.1
12	33.39	8.69	27.75	1106.3	37.5	25	26.6	41.22	50.45
10	31.4	8.85	28.96	1154.6	37.5	25	26.6	41.32	49.26
8	29.45	9.13	30.56	1218.2	37.5	25	26.6	41.31	47.91
6	28.03	9.56	32.71	1304	37.5	25	26.6	41.17	45.16
4	26.96	10	36.21	1443.2	37.5	25	26.6	40.56	43.55
2	24.66	12	39.53	1576	37.5	25	26.6	39.56	41.84
0	20.03	13	41.83	1667.4	37.5	25	26.6	38.7	36.91

Table 3. *Specifications for the Proposed Combined Cycle.*

HRSG (1) Stack temperature, $T_e = 170.25$ ℃ (2) Saturation temperature in Evaporator $T_5 = 250.3$ ℃ (3) Pinch point temperature difference Δ_{tpp}= 10 ℃ (4) HRSG Heat Load $Q_{HRSG} = 38.49\ MW$ (5) HRSG Thermal Ratio $\eta_{HRSG} = 0.85$ (6) Heat rejected by exhaust gas: $\dot{Q}_{ea} = 45.28\ MW$ (7) Heat loss $H_L = 6.79\ MW$	Steam Turbine (1) Inlet temperature $T_1 = 450$ ℃ (2) Steam saturation pressure $P_1 = 40\ bar$ (3) Isentropic efficiency $\eta_{is} = 89.06$ % (4) Thermal efficiency $\eta_{th} = 31.40$ % (5) Power output $P_{ST} = 16.38MW$ (6) Mass flow rate $\dot{m}_s = 14.45\ kg/s$ (7) Specific steam consumption $S.S.C = 8.85\ kg/kWh$ (8) Steam outlet pressure (condenser pressure) $P_2 = 0.1\ bar$ (9) Steam outlet temperature (condenser temperature) $T_2 == 45.8$ ℃ (10) Condenser Heat Load $\dot{Q}_3 = 28.96\ MW$ (11) Feed pump Load $P_P = 0.06\ MW$
Steam Turbine Generator (1) Power output $P_{Net_{ST}} = 16.32\ MW$ (2) Thermal efficiency $\eta_{gen} = 31.40$ % Condenser Cooling Water Parameters (1) Inlet temperature $t_{in} = 29.8$ ℃ (2) Outlet temperature $t_{out} = 35.8$ ℃ (3) Mass flow rate $\dot{m}_w = 1154.6\ kg/s$ (4) Condenser Thermal Ratio $\eta_{cond} = 0.375$	Combined Cycle Analysis (1) Overall power output $P_{CC} = 41.32\ MW$ (2) Overall efficiency $\eta_{CC} = 49.26$ %

4. Discussion

The following discussions were deduced from the analysis based on result:

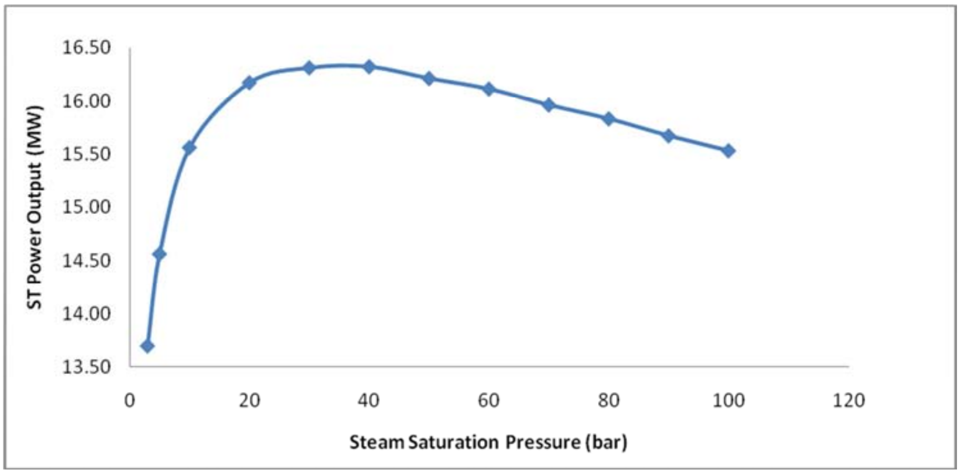

Figure 9. *Effect of Steam Saturation Pressure on ST Power Output.*

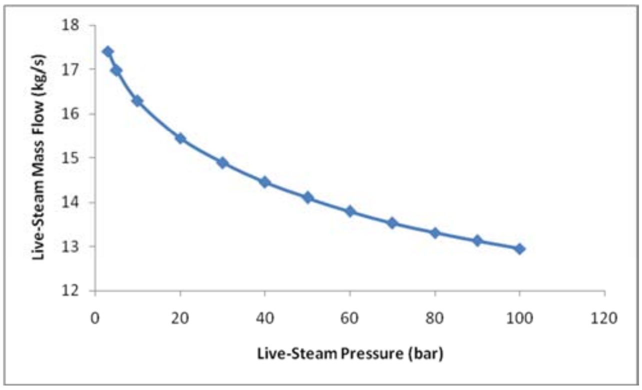

Figure 10. *Effect of Live-Steam Pressure on Live-Steam Mass Flow.*

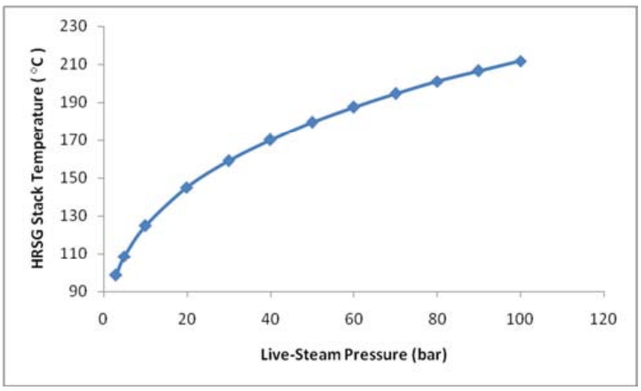

Figure 11. *Effect of Live-Steam Pressure on HRSG Stack Temperature.*

the analysis based on result:

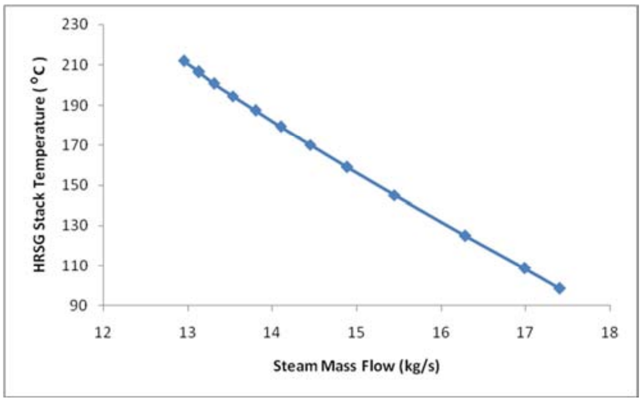

Figure 12. *HRSG Stack Temperature Vs Live-Steam Mass Flow.*

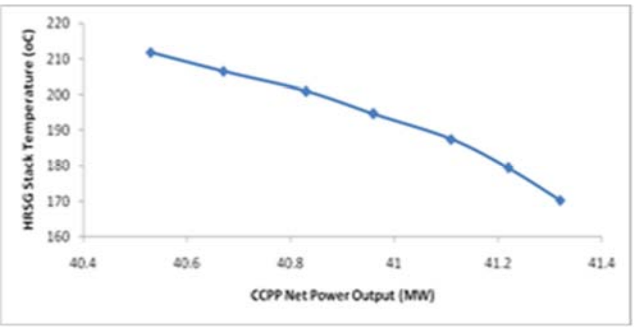

Figure 13. *Effect of HRSG Stack Temperature CCPP Net Power Output.*

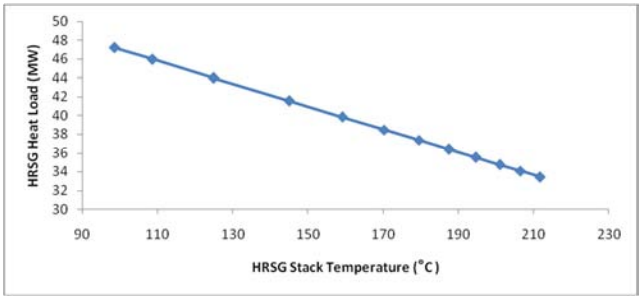

Figure 14. *HRSG Stack Temperature Vs HRSG Heat Load.*

Figure 9 shows that as the steam saturation pressure decreases, the steam turbine power output increases and converge at a maximum of 16.32 MW corresponding to a steam saturation pressure of 40 bar after which it started declining.

Figure 10 shows the effect of live steam pressure on the live-steam mass flow rate, indicating that the live steam mass flow increases with a decreasing live steam pressure. The results show that to generate more steam, the live steam pressure should be reduced.

Figure 11 illustrates the effect of live steam pressure on HRSG stack temperature. It shows that at lower live steam pressure, there is a lower HRSG stack temperature indicating that exhaust gas is well utilized. However, the HRSG stack temperature should not be reduced below the acid dew point of the flue gas which is about 160°C maximum. Hence, HSRG stack temperature of 170.25°C was chosen, corresponding to 40 bar.

Figure 12 shows the influence of the HRSG stack temperature on live steam mass flow. It shows an increase in live steam mass flow for every decrease in HRSG stack temperature. To increase steam production, the HRSG stack temperature should be cooled as much as possible but not below 160°C being the acid dew point of the flue gas, which may condense and corrode the components. In this analysis, the HRSG stack temperature of 170.25°C corresponds to a live steam mass flow of 14.45 kg/s was chosen.

Figure 13 shows that as the HRSG stack temperature decreases, the CCPP net power output increases. This indicates that much heat will be extracted as HRSG stack temperature reduces leading to increased steam production which will result to increase in steam turbine power output. The resultant effect of these is the increase in the CCPP net power output.

Figure 14 shows that as the HRSG stack temperature reduce, the HRSG heat load increases. This implies that, to effectively harness heat from the HRSG, the stack temperature should be greatly reduced. This in turn increases the live steam mass flow resulting to a larger HRSG heat load.

Figure 15 shows that for every increase in the live steam mass flow, there is a corresponding increase in the steam turbine power output. This is because an increase in mass flow results to an increased HRSG capacity (input) leading to an increased output in the steam turbine. Again, since the steam turbine output is a product of mass flow and enthalpy change, any positive change in mass flow will bring about a positive change in the steam turbine output.

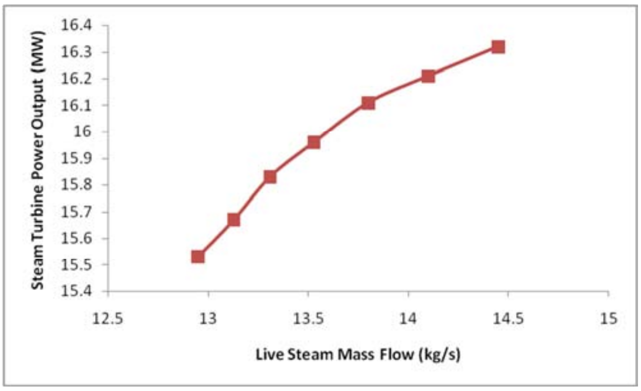

Figure 15. *Effect of Live-Steam Mass Flow on Steam Turbine.*

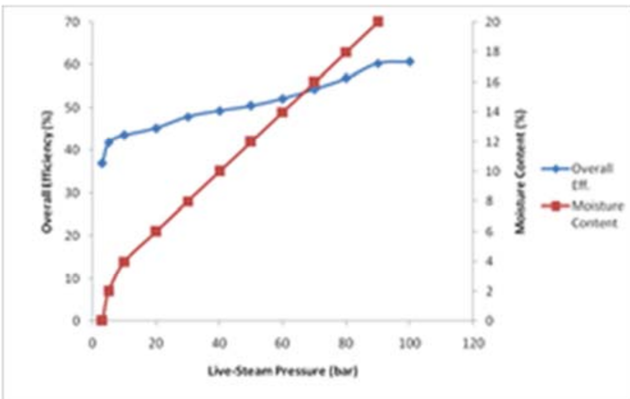

Figure 16. *Effect of Live-Steam Pressure on Overall Efficiency.*

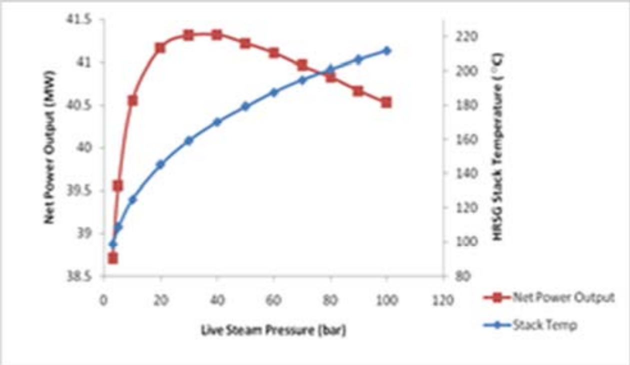

Figure 17. *Effect of Live-Steam Pressure on Net Power Output and Power Output and Steam Turbine Exhaust Moisture Content HRSG Stack Temperature*

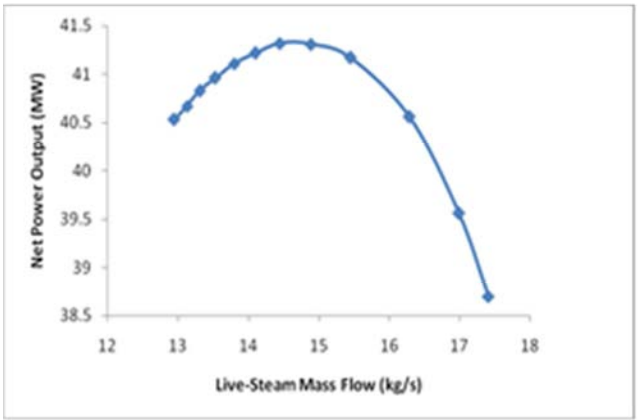

Figure 18. *Effect of Live-Steam Mass Flow on Net Power Output.*

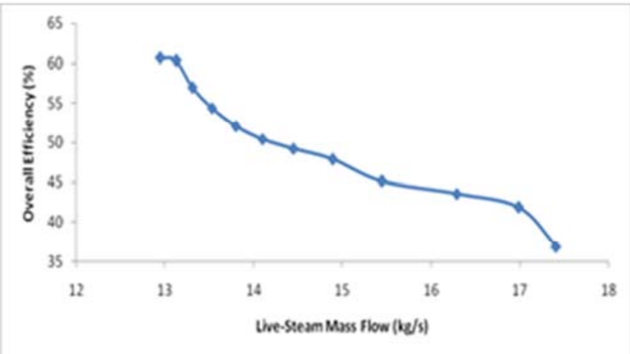

Figure 19. *Effect of Live-Steam Mass Flow on Overall Efficiency.*

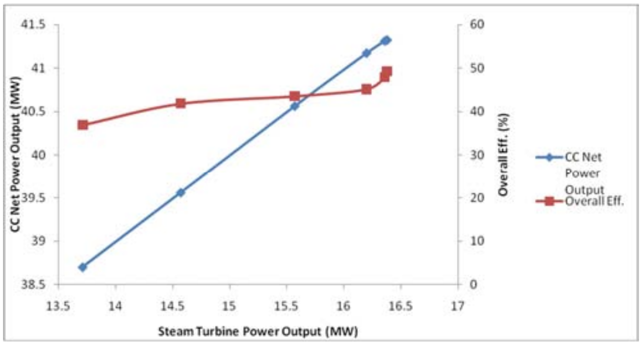

Figure 20. *Effect of Steam Turbine Power Output on CC Power Output and Overall Efficiency.*

Figure 16 shows the effect of live-steam pressure on overall efficiency and steam turbine exhaust moisture content. Observation shows a steady increase in the overall efficiency as the live steam pressure increases. This is an indication that a highly efficient performance of the combined cycle plant will be attained at a very high pressure. However, for the 25 MW gas turbine, the live steam pressure cannot be continuously increased just for the purpose of having the highest possible efficiency as this will have a negative impact on the power output which has a diminishing return around 40 bar. Another negative aspect of a higher live steam pressure in a single pressure cycle is an increase in the moisture content at the end of the steam turbine. A high moisture content increases the risk of erosion at the last stages of the turbine. A limit of moisture content is set at about 16% and or a dryness fraction of 0.87. Hence, for economic reasons, current gas turbines are generally optimized with respect to maximum power density (output per unit air flow) rather than efficiency [18]. From the analysis in Table 2, the chosen live steam pressure of 40 bar corresponds to the maximum net power output of 41.32 MW which coincides with an acceptable moisture content of 10%.

Figure 17 shows the effect of live-steam pressure on net power output and HRSG stack temperature. For the live steam pressures between 100 bar to 3 bar, there is an increase in the net power output and a peak at 40 bar where the net power output has its maximum of 41.32 MW. This also coincides with an acceptable HRSG stack temperature of 170.25°C which is above the acid dew point of the flue gas. Beyond the maximum point, there is a progressive decline in the net power output with further increase in the live steam pressure. This point was chosen as the design point for the combined cycle power plant.

Figure 18 illustrates the effect of live-steam mass flow on net power output. The graph shows that as the live steam mass flow increases, the net power output increases as well. However, the net power output peaks at 41.32 MW which is the maximum value attainable in the analysis and at a live steam mass flow of 14.45 kg/s. This implies that for the 25 MW gas turbine with for an exhaust gas temperature of 487°C, maximum power output is attained at a mass flow of 14.45 kg/s, at an optimum pressure of 40 bar within the range live steam pressures from 3 bar to 100 bar.

From Figures 17 and 18, it can be deduced that the best combination of process parameters of steam leaving the steam generator that will give the optimum performance of the combined cycle plant is determined at 40 bar and 14.45 kg/s.

Figure 19 shows that the overall efficiency gradually drops with a steady increase in the live steam mass flow rate. However, it is observed that a reasonable efficiency of 49.26% is obtained at the live steam mass flow of 14.45 kg/s attained at the maximum power output of 41.32 MW.

Figure 20 shows that the steam turbine power output steadily increases with a progressive increase in combined cycle net power output and overall efficiency. It indicates that the retrofitting of the steam turbine improves the performance.

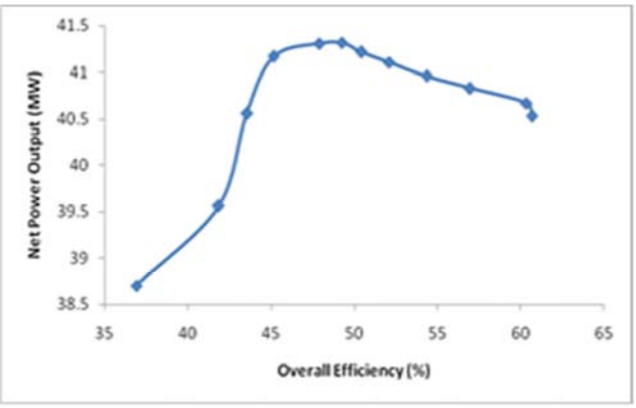

Figure 21. *Relationships between Net Power Output and Overall Efficiency.*

Figure 21 shows the relationships between net power output and overall efficiency of the combined cycle plant. It shows that the net power output steadily increase with the overall cycle efficiency until a maximum point of 41.32 MW is reached where the net power output peaked, thereafter; there is a diminishing return in the output power. However, this optimum point of the output power coincides with a reasonable efficiency of 49.26% for the combined cycle plant.

5. Conclusion and Recommendation

The general results from the analysis in Table 2 and discussion showed that the maximum points of 16.32 MW and 41.32 MW for the steam turbine power output and CCPP power output respectively, are the maximum values within the required range of the proposed steam turbine as well as CCPP. Again, this point, corresponds to an acceptable HRSG stack temperature of 170.25°C which is above the acid dew point of flue gas as required and a live steam mass flow and pressure of 14.45 kg/s and 40 bar respectively, with an acceptable steam turbine exhaust moisture content of 10%. The 7^{th} iteration is therefore chosen for the combined cycle design of the Omoku gas turbine power plant. Table 3 shows the detailed specification of the required 16.32 MW steam turbine output (attained from the 7^{th} iteration of Table 2) for the combined cycle power plant. This 16.32 MW steam turbine power output attained at a mass flow of 14.45kg/s results from the 124.1 kg/s of exhaust gas at an EGT of 487°C of the Omoku gas turbine indicating that 1kg of exhaust gas will produce 0.1164 kg of steam.

Deductions from all the analysis and discussions resulted to a combined cycle power output of 41.32 MW with an overall efficiency of 49.26%. This higher efficiency of the combined cycle achieved compared with that of the dry mode Omoku gas turbine of 26.6% indicates that the amount of emissions discharged into the atmosphere per unit mass of fuel burnt is less. Again, the lower stack temperature of 170.25°C from this proposed combined cycle plant compared with the exhaust gas temperature of 487°C of the existing Omoku gas turbine indicate a reasonable reduction in the waste heat intensity to the environment. Thus, the CCS generates about 65.30% boost in the net power output, 85.20% improvement in overall efficiency and 65.10% reduction in waste heat intensity to the environment, thereby contributing to reduction in thermal pollution hence, global warming. Hence, the work showed that for the design of a CTPP with a single pressure level HRSG without supplementary firing, a recommended range for the power output of the steam bottoming plant falls within 34 – 40% of the total power output of the CTPP while that of the gas topping plant falls within the range of 60 – 66% of the total power output of the CTPP, thereby validating the analysis of Ragland *et al*., [20].

Therefore, the results from retrofitting the Omoku GT with a steam turbine demonstrate an effective utilization of waste heat from the Omoku gas turbine plant for energy recovery as more power is generated at a higher efficiency, as well as reduction in the waste heat intensity to the environment. In effect, the plant performance is enhanced.

Hence, this research confirms the viability as well as demonstrates the application, of the combined cycle concept for the Omoku gas turbine. It thus enhances the usefulness of this engine as it presents to manufacturers and users, the feasibility of converting this engine and similar engines to a combined cycle.

It is therefore recommended that further research should be carried out on how to introduce a multiple pressure level HRSG with supplementary firing to the combined cycle system for an improved efficiency and output.

Nomenclature

Symbol	Description	Unit
c	Specific heat	kJ/kgK
Cp	Specific heat at constant pressure	kJ/kgK
c_{peg}	Specific heat of exhaust gas at constant pressure	kJ/kgK
c_{pw}	Specific heat of water	kJ/kgK
c_{p_s}	Specific heat of steam at constant pressure	kJ/kgK
h	Enthalpy	kJ/kg
h_1	Enthalpy at steam turbine inlet	kJ/kg
h_2	Enthalpy at steam turbine outlet	kJ/kg
h_3	Enthalpy at condenser outlet	kJ/kg
h_4	Feed water enthalpy	kJ/kg
h_5	Enthalpy at economizer exit	kJ/kg
h_6	Enthalpy at evaporator exit	kJ/kg
H_L	Heat loss	MW

Symbol	Description	Unit
$\dot{m}_{eg}$	Mass flaw rate of exhaust gas	kg/s
$\dot{m}_{w}$	Mass flow rate of cooling water	kg/s
$\dot{m}_{s}$	Mass flow rate of steam	kg/s
p	Pressure	bar
P	Power	MW
P_1	Steam saturation pressure	bar
P_2	Condenser Inlet pressure	bar
P_3	Condenser Outlet/Feed Pump Inlet pressure	bar
P_4	Feed Pump Outlet pressure	bar
P_C	Compressor Power	MW
P_T	Turbine Power	MW
P_{CC}	Combined cycle power output	MW
$P_{NET_{gT}}$	Gas turbine net power output	MW
$P_{NET_{ST}}$	Steam turbine net power output	MW
P_P	Pump power input	MW
P_{ST}	Steam turbine power output	MW
q_{in}	Heat flow in	kJ/kg
q_{out}	Heat flow out	kJ/kg
Q	Heat flow	kW
$\dot{Q}_1$	Heat Supplied	MW
$\dot{Q}_2$	Heat Rejected	MW
$\dot{Q}_3$	Heat rejected in Condenser (Condenser Heat Load)	MW
$\dot{Q}_{eg}$	Heat rejected by exhaust gas	MW
Q_{HRSG}	Heat recovered by HRSG (HRSG Heat Load)	MW
s	Entropy	kJ/kgK
T	Temperature	°C / K
T_a	Compressor Inlet Temperature	°C
T_d	Gas Turbine Exhaust Temperature	°C
T_e	HRSG Stack Temperature	°C
T_1	Steam Turbine Inlet Temperature	°C
T_2	Condenser saturated temperature	°C
T_5	Steam saturation temperature	°C
T_x	Temperature of exhaust gas at pinch point	°C
t_{in}	Temperature of cooling water into condenser	°C
t_{out}	Temperature of cooling water out of the condenser	°C
W_{net} Symbol	Description	Unit
c	Specific heat	kJ/kgK
Cp	Specific heat at constant pressure	kJ/kgK
c_{peg}	Specific heat of exhaust gas at constant pressure	kJ/kgK
c_{p_w}	Specific heat of water	kJ/kgK
c_{p_s}	Specific heat of steam at constant pressure	kJ/kgK
h	Enthalpy	kJ/kg
h_1	Enthalpy at steam turbine inlet	kJ/kg
h_2	Enthalpy at steam turbine outlet	kJ/kg
h_3	Enthalpy at condenser outlet	kJ/kg
h_4	Feed water enthalpy	kJ/kg
h_5	Enthalpy at economizer exit	kJ/kg
h_6	Enthalpy at evaporator exit	kJ/kg
H_L	Heat loss	MW
$\dot{m}_{eg}$	Mass flaw rate of exhaust gas	kg/s
$\dot{m}_{w}$	Mass flow rate of cooling water	kg/s
$\dot{m}_{s}$	Mass flow rate of steam	kg/s
p	Pressure	bar
P	Power	MW
P_1	Steam saturation pressure	bar
P_2	Condenser Inlet pressure	bar
P_3	Condenser Outlet/Feed Pump Inlet pressure	bar
P_4	Feed Pump Outlet pressure	bar
P_C	Compressor Power	MW
P_T	Turbine Power	MW
P_{CC}	Combined cycle power output	MW
$P_{NET_{gT}}$	Gas turbine net power output	MW
$P_{NET_{ST}}$	Steam turbine net power output	MW
P_P	Pump power input	MW
P_{ST}	Steam turbine power output	MW
q_{in}	Heat flow in	kJ/kg

Symbol	Description	Unit
q_{out}	Heat flow out	kJ/kg
Q	Heat flow	kW
$\dot{Q}_1$ Heat Supplied	MW	
$\dot{Q}_2$	Heat Rejected	MW
$\dot{Q}_3$	Heat rejected in Condenser (Condenser Heat Load)	MW
$\dot{Q}_{eg}$	Heat rejected by exhaust gas	MW
Q_{HRSG} Heat recovered by HRSG (HRSG Heat Load)	MW	
s	Entropy	kJ/kgK
T	Temperature	°C / K
T_a	Compressor Inlet Temperature	°C
T_d	Gas Turbine Exhaust Temperature	°C
T_e	HRSG Stack Temperature	°C
T_1 Steam Turbine Inlet Temperature	°C	
T_2 Condenser saturated temperature	°C	
T_5	Steam saturation temperature	°C
T_x	Temperature of exhaust gas at pinch point	°C
t_{in}	Temperature of cooling water into condenser	°C
t_{out}	Temperature of cooling water out of the condenser	°C
W_{net} Net work output	kJ/kg	
W_T	Turbine work	kJ/kg
W_{ST}	Steam turbine work	kJ/kg
W_P	Pump work	kJ/kg
W_{gt}	Gas turbine work	kJ/kg
Net work output	kJ/kg	
W_T	Turbine work	kJ/kg
W_{ST}	Steam turbine work	kJ/kg
W_P	Pump work	kJ/kg
W_{gt}	Gas turbine work	kJ/kg
Greek Symbols		
ΔT_p	Pinch point temperature difference	°C
ΔT_a	Approach temperature difference	°C
η	Efficiency,,	%
η_c	Compressor isentropic efficiency	%
η_{CC}	Combined cycle overall efficiency	%
η_{cond}	Condenser efficiency	%
η_{gT}	Gas turbine thermal efficiency	%
η_{HRSG} HRSG Thermal ratio	%	
η_{ST}	Steam turbine thermal efficiency	%
η_{th}	Thermal efficiency	%
Subscripts		
g	Gas	
is	Isentropic	
in	Inlet	
out	Outlet	
p	At constant pressure	
th	Thermal	
Abbreviations		
CC	Combined Cycle	
CCPP	Combined Cycle Power Plant	
CCS	Combined Cycle System	
CO_2	Carbondioxide	
CTPP	Combined Thermal Power Plant	
DP	Design Point	
EGT	Exhaust Gas Temperature	
GE	General Electric	
GT	Gas Turbine	
GTC	Gas Turbine Cycle	
HMI	Human Machine Interface	
HRSG	Heat Recovery Steam Generator	
Kw	Kilo Watts	
Kg	Kilo Gram	
LHV	Lower Heating Value	
Mpa	Mega Paschal	
MW	Mega Watts	
NO_X	Nitrogen Oxide	
OD	Off-Design Point	

RSTC	Retrofitted Steam Turbine Cycle
SSC	Specific Steam Consumption
ST	Steam Turbine
WGS	World Geodetic System

References

[1] Le-ol, A. K. (2016) Improvement of Omoku Gas Turbine Power Plant for Combined Cycle Operation. M. Tech. Dissertation, Department of Mechanical Engineering, Rivers State University, Port-Harcourt, Nigeria.

[2] Kumar, P. (2010) Optimization of Gas Turbine Cycle Using Optimization Technique. M. Eng. Thesis, Department of Mechanical Engineering, Thapar University, Patiala-147004, India.

[3] Aref, P. (2012) Development of Framework for Thermo-Economic Optimization of Simple and Combined Gas Turbine Cycles; Ph. D. Thesis, school of Engineering, Cranfield University.

[4] Rao, S. and Parulekar, B. B. (2007) Energy Technology: Non-Conventional, Renewable and Conventional. Khanna Publishers, Naisarak, Delhi.

[5] Lebele-Alawa, B. T. and Le-ol, A. K. (2015) Improved Design of a 25 MW Gas Turbine Plant using Combined Cycle Application Journal of Power and Energy Engineering, 3, 1-14 http://dx.doi.org/10.4236/jpee.2015.38001.

[6] De, S., Nag, P. K. (2000) Effect of Supplementary Firing on the Performance of an Integrated Gasification Combined Cycle Power Plant. Indian Institute of Technology, Kharagpur, India, Proc. Instn. Mech. Engrs., 214, Part A.

[7] Kehlhofer, R., Rukes, B., Hannemann, F., & Stirnimann, F. (2009) Combined-Cycle Gas & Steam Turbine Power Plants, PenWell Corporation, Third Edition, Tulsa, Oklahoma, USA.

[8] Nickhil, D., Sansher, S. S. Kachhwaha, Rajesh, A. A. (2012) Review of Combined Cycle Power Plant Thermodynamic Cycles: Proceedings of the National Conference on Trends and Advances in Mechanical Engineering, YMCA University of Science and Technology, Faridabad, Haryana, Oct. 19-20.

[9] Lars, O. N. & Bolland, O. (2012) Steam Bottoming Cycles Offshore – Challenges and Possibilities. Journal of Power Technologies, 92 (3), 201-207.

[10] Polyzakis A. L., Koroneous C., & Xydis G., (2008) Optimum Gas Turbine Cycle for Combined Cycle Power Plant. Energy Conversion and Management Publications 49, 551-563.

[11] Tiwari, A. K, Hasan, M. M, Islam, M. (2012) Effect of Operating Parameters on the Performance of Combined Cycle Power Plant.1: 351 doi: 10.4172/scientificreports.

[12] Ravi Kumar, N., Rama Krishna, K., & Sita Rama Raju, A. V. (2006) Performance Simulation of Heat Recovery Steam Generator in Combined Cycle Power Plant. Proceeding of the 18th National and 17th ISHMT-ASME Heat and Mass Transfer Conference, India.

[13] Murad, A. R., Amirabedin, E., Yilmazoglu, M. Z., & Durmaz, A. (2010) Analysis of Heat Recovery Steam Generators in Combined Cycle Power Plants. The Second International Conference on Nuclear and Renewable Energy Resources, Ankara, Turkey.

[14] Ahmed, S. Y. (2013) Performance of the Combined Gas Turbine-Steam Cycle for Power Generation. Mathematical Theory and Modeling, 3, 12.

[15] Thamir, K. I. & Rahman, M. M. (2012) Effect of Compression Ratio on Performance of Combined Cycle Gas Turbine: Scientific & Academic Publishing. International Journal of energy Engineering; 2 (1), 9-14.

[16] Service Manual (Gas Turbine MS 5001) of 25 MW Unit of Omoku Power Generation Station. GEPS Oil & Gas, Nuovo Pignone, Volume 1; G. T Description, Instruction & Operation.

[17] Armando, A. (2013) Optimization of Maputo Power Plant, Master of Science Thesis, KTH School of Industrial Engineering and Management Energy Technology, STOCKHOLM.

[18] Kehlhoffer, R. (1997) Combined Cycle Gas and Steam Turbine Power Plants. PennWell Publishing Company, Oklahoma.

[19] Jehar and Associates. Introduction to HRSG design. www.hrsgdesign.com.

[20] Ragland, A., Vogt-NEM, Stenzel, W. (2000) Combined Cycle Heat Recovery Optimization. Proceedings of 2000 International Joint Power Generation Conference, Miami Beach, July 23 (26), 1781-1787.